Medical Physics
The International Journal of Medical Physics Research and Practice

In vivo motion and force measurement of surgical needle intervention during prostate brachytherapy

Tarun Podder, Douglas Clark, Jason Sherman, Dave Fuller, Edward Messing, Deborah Rubens, John Strang, Ralph Brasacchio, Lydia Liao, Wan-Sing Ng, and Yan Yu

Citation: Medical Physics **33**, 2915 (2006); doi: 10.1118/1.2218061
View online: http://dx.doi.org/10.1118/1.2218061
View Table of Contents: http://scitation.aip.org/content/aapm/journal/medphys/33/8?ver=pdfcov
Published by the American Association of Physicists in Medicine

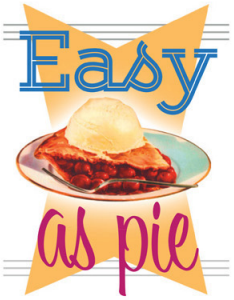

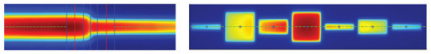

In vivo motion and force measurement of surgical needle intervention during prostate brachytherapy

Tarun Podder,[a] Douglas Clark, Jason Sherman, and Dave Fuller
Department of Radiation Oncology, University of Rochester Medical Center, Rochester, New York 14642

Edward Messing
Departments of Radiation Oncology and Surgery, University of Rochester Medical Center, Rochester, New York 14642

Deborah Rubens
Departments of Radiology and Surgery, University of Rochester Medical Center, Rochester, New York 14642 and Department of Biomedical Engineering, University of Rochester, Rochester, New York 14642

John Strang
Department of Radiology, University of Rochester Medical Center, Rochester, New York 14642

Ralph Brasacchio
Department of Radiation Oncology, University of Rochester Medical Center, Rochester, New York 14642

Lydia Liao
Departments of Radiology and Radiation Oncology, University of Rochester Medical Center, Rochester, New York 14642

Wan-Sing Ng
School of Mechanical and Aerospace Engineering, Nanyang Technological University, Singapore 639798

Yan Yu
Department of Radiation Oncology, University of Rochester Medical Center, Rochester, New York 14642 and Department of Biomedical Engineering, University of Rochester, New York 14642

(Received 15 September 2005; revised 2 June 2006; accepted for publication 4 June 2006; published 25 July 2006)

In this paper, we present needle insertion forces and motion trajectories measured during actual brachytherapy needle insertion while implanting radioactive seeds in the prostate glands of 20 different patients. The needle motion was captured using ultrasound images and a 6 degree-of-freedom electromagnetic-based position sensor. Needle velocity was computed from the position information and the corresponding time stamps. From *in vivo* data we found the maximum needle insertion forces to be about 15.6 and 8.9 N for 17 gauge (1.47 mm) and 18 gauge (1.27 mm) needles, respectively. Part of this difference in insertion forces is due to the needle size difference (17G and 18G) and the other part is due to the difference in tissue properties that are specific to the individual patient. Some transverse forces were observed, which are attributed to several factors such as tissue heterogeneity, organ movement, human factors in surgery, and the interaction between the template and the needle. However, theses insertion forces are significantly responsible for needle deviation from the desired trajectory and target movement. Therefore, a proper selection of needle and modulated velocity (translational and rotational) may reduce the tissue deformation and target movement by reducing insertion forces and thereby improve the seed delivery accuracy. The knowledge gleaned from this study promises to be useful for not only designing mechanical/robotic systems but also developing a predictive deformation model of the prostate and real-time adaptive controlling of the needle. © *2006 American Association of Physicists in Medicine*.
[DOI: 10.1118/1.2218061]

Key words: prostate brachytherapy, needle insertion force, robotic needle intervention, *in vivo* force, surgical needle insertion, prostate seed implantation

I. INTRODUCTION

Numerous medical diagnostic and therapeutic procedures, e.g., tissue biopsy, brachytherapy, blood/fluid sampling, abscess drainage, deep brain biopsy, etc., require percutaneous insertion of surgical needles. Accurate placement of needle in these procedures is very important. However, accurate steering and placement of different types of surgical needles in soft tissues are challenging for several reasons such as tissue heterogeneity, anisotropy, nonlinear elastic stiffness, relaxation, unfavorable anatomic structures, needle bending, inadequate sensing, tissue deformation and deflection, and poor maneuverability. Therefore, understanding the complex mechanism of needle interaction with living soft tissue is an area of active research.

In brachytherapy, positional accuracy of the radioactive seeds is very important for optimizing the dose delivery to the targeted tissues, sparing the critical organs and structures. In currently practiced procedures, the fixed grid holes in the template allow the surgeon to insert the needle at specified fixed positions. Very little can be done to steer the needles to a place other than these specific locations. However, alterations in needle insertion position may be required based on intraoperative dynamic planning. Sometimes, especially for larger prostates, it is required that the needle be angulated to avoid pubic arch interference (PAI) and gain access to the desired target position in the prostate for seed delivery. In the conventional brachytherapy procedure with a fixed template, needle angulation is almost impossible, although the surgeon can manually bend the needle and get to the desired position after several trials. It appears that robot-assisted needle intervention can significantly improve accuracy and consistency of various medical procedures.

Recently, several researchers have developed robotic systems for permanent seed implant (PSI) in the prostate.[1–6] To design and control any robotic system, the design and control engineers must know the robotic workspace, motion profile, and force-torque that will be encountered by the system. Especially for prostate brachytherapy procedures for implanting radioactive seeds, the workspace analysis and the assessment of force-torque encountered by the needle insertion mechanism are critical mainly due to (1) the limited lateral space available between two legs of the patient (when on the operating room (OR) table in lithotomy position) in order to insert a needle transperinually, and (2) the needle must penetrate through several layers of different types of tissue (skin, perineal muscles, bulbospongiosus tissue, fascia tissue, prostate capsule, prostate tissue, etc.[7]), which exert variable forces.

The surface of the perineal wall through which the needles are inserted during the PSI is about 6×6 cm^2 and the maximum area of the robot workspace projected on the perineal wall ranges from about 8×8 cm^2 to 12×12 cm^2 (considering the drape on the patient's body). Thus, the workspace for the robotic system with needle insertion mechanism is quite limited. To develop a robotic system that can work effectively in this constrained space, requires compact design of components and judicial selection of motors and accessories. On the other hand, the system's rigidity and factor of safety should not be compromised in order to make the system compact. Therefore, to design an optimal system, it is important to know the maximum force that the needle may encounter during insertion into the patient. Thus, *in vivo* measurement of needle insertion force is very useful in designing and controlling any robotic system that will work in such a limited space.

Several researchers have reported needle insertion forces and developed soft tissue models while the insertions have been performed mainly in soft material phantoms like polyvinylchloride (PVC),[8–10] silicon rubber,[11,12] and *ex vivo* animal tissues such as bovine liver,[12–15] porcine liver,[16,17] chicken breast,[18] and canine prostate.[19]

Some empirical as well as analytical models of needle insertion forces have been reported by various researchers.[8,11–19] DiMaio *et al.*[8] have developed analytical models for estimating needle forces and soft tissue deformation using the finite element model (FEM) with linear elastic modulus. Although their simulation results reasonably matched with experimental data while inserting the needle into PVC phantom, they have pointed out that the models might not be amenable to real-time simulation or agreeable with *in vivo* measurement. Several investigators have compared the simulation results obtained from these models with the measured forces during needle insertion into bovine livers.[14,15] The overall shape of the model data is similar to the measured data, but they have concluded that perfect match is impossible because of the significant variations in liver geometry and internal structure of the liver.

Some mechanical properties such as modulus of elasticity (Young's modulus), Poisson's ratio, relaxation, stress, and strain, measured from *ex vivo* human tissues, are also available in the literature.[20–25] Some of these properties are being used to develop various models, including the FEM. However, the vast majority of research on mechanical properties of tissues has been done for tissues that are subject, actively or passively, to some degree of mechanical activity (muscles, arteries, lungs, tendons, bones, skin, urethra). In contrast, very little quantitative information is available on the elastic property of the tissue in organs that do not have mechanical activity (breast, prostate, thyroid, testes, etc.).[20] Using uniaxial and biaxial tests on *ex vivo* soft tissues such as the breast tissue, skin, and ureteral muscle, Fung[21] and Wellman *et al.*[22] have shown that they exhibit very significant nonlinear behavior. Krouskop *et al.*[20] measured the Young's modulus of 142 breast tissues and 113 prostate tissues from *ex vivo* specimens under various compression levels, and noted that the modulus values increase significantly as a result of increasing the precompression load. Since these experiments are fundamentally different from the needle insertion experiments, the results cannot be compared. Matsumiya *et al.*[25] have analyzed forces during robotic needle insertion to human vertebra, which is a hard tissue; it is quite different from needle insertion into soft tissue. Interestingly they have found that the forces during robotic insertion to human femoral head are 50% less than those during manual insertion and they have indicated that the robot can contribute to safe needle insertion to human vertebra in percutaneous vertebroplasty.

Although *ex vivo* measurement can be more accurate for a small piece of sample, there are two main differences between *ex vivo* and *in vivo* measurements, especially for PSI: (1) during *in vivo*, i.e., actual brachytherapy in the OR, the needle traverses through different types of tissues/organs having nonlinear viscoelastic properties, and (2) factors such as the boundary conditions acting on the organ, organ/tissue interface, blood flow, temperature and humidity differences, etc. None of these issues can be resolved accurately using current state-of-the-art methodologies and technologies.

Perhaps none of the existing models, either empirical or analytical including FEM, along with *ex vivo* measurements

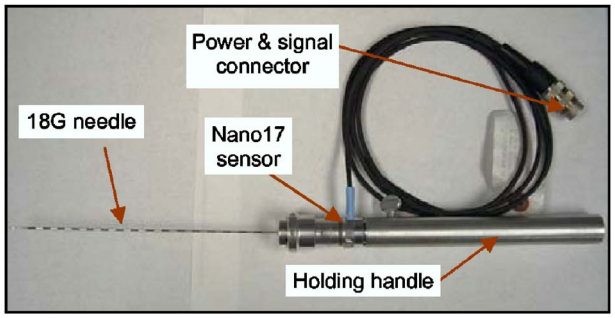

FIG. 1. Hand-held adapter.

can accurately assess the forces and tissue deformations while the needle is inserted into the prostate transperineally. But, to the best of our knowledge, to date no *in vivo* force measurement data for needle insertion in human soft tissue, especially in prostate gland, have been reported. Therefore, in this study we have measured and quantified *in vivo* needle insertion forces and motion profiles during prostate brachytherapy in the OR, which helped us in designing and controlling our Endo-Uro Computer Lattice for Intratumoral Delivery, Implantation, and Ablation with Nanosensing (EUCLIDIAN).

II. MATERIALS AND METHODS

We have acquired needle insertion force-torque (F-T) and motion profile data from 20 different patients during prostate brachytherapy in the OR using a hand-held adapter (Figs. 1 and 2). The adapter that we have developed is equipped with a 6 DOF F-T sensor Nano17® (ATI Industrial Automation, Apex, NC) and a 6 DOF electromagnetic (EM)-based position sensor miniBIRD® (Ascension Technology Corporation, Burlington, VT). The miniBIRD® was attached to the hand-held adapter to measure 3D positions and orientations of the needle and the corresponding time stamps are recorded automatically for calculating the needle insertion velocity. To have synchronized data, we have integrated EM-based position sensor (miniBIRD®) with the F-T sensor (Nano17®) so that F-T sensor can trigger the position sensor. Additionally, the needle progression into the soft tissue (perineum, prostate, and other organs) and prostate deformation and movement have been recorded using ultrasound (Acuson™ 128xP, Mountain View, CA) imaging technique.

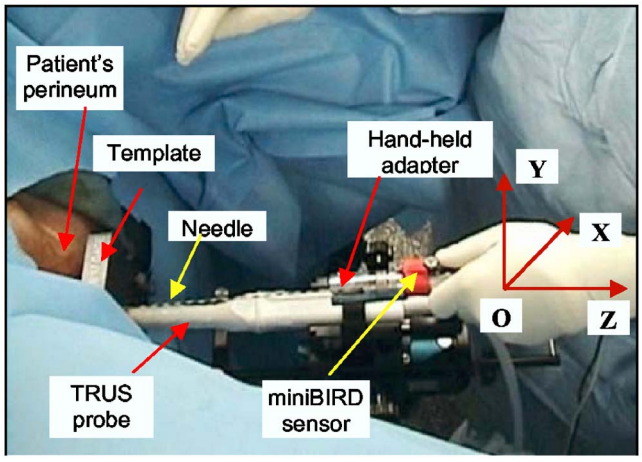

FIG. 2. Force/torque and position data collection during actual brachytherapy procedure in the OR.

Data were collected under a Research Subject Review Board approved protocol and with patient's informed consent. Commercially available brachytherapy needles having 1.47 mm (17G) and 1.27 mm (18G) diameter and 200 mm length with diamond tip trocars (Mick Radio-Nuclear instruments, Inc., NY) were used. There were 25 17G needle insertions in ten patients and 27 18G needle insertion in another ten patients with two to three insertions per patient. Only one type of needle (either 17G or 18G) was used for each of the patients. Of the 20 patients, for 18 patients the hand-held F-T adapter was operated by an experienced surgeon having more than 30 years of surgical experience and 8 years of PSI experience. The other two patients were treated by another surgeon having about 3 years of PSI experience. An experienced radiologist captured the transrectal ultrasound images, in the sagittal plane, of the needle progression through various tissues and organs. The time, position, and force data during needle insertion were recorded at a frequency of 100 Hz.

III. RESULTS AND DISCUSSION

Selection of the needle size (17G or 18G) during a PSI procedure is based on certain patient-specific criteria and the physical properties of the needle. For instance, if the patient receives prior hormonal therapy or external beam radiation treatment (EBRT), then the prostate becomes harder which, in turn, requires a stiffer needle to reduce undesirable deviation of the needle from the desired trajectory. The other important criteria are the hardness and thickness of the skin of the patient and special anatomic conditions. The thicker or harder the skin, the stiffer the needle required, therefore a 17G needle is used because of its larger diameter (another option could be the use of stronger material, but no such needle is commercially available or cost prohibitive). Use of an 18G needle is preferable due to the fact that it creates less trauma, edema, and tissue/organ deformation or movement. However, the surgeon decides the needle based on the patient's conditions and with informed knowledge of the properties of the needle.

Here, we present a representative case of a single needle insertion forces, torques, positions, and velocities into one patient for 18G needle (Fig. 3) and into another patient for 17G needle (Fig. 4), for a total of 52 needle insertions into 20 patients. Since after insertion the needle needs to be in the patient for delivering seeds, we have not presented force data during hand-held adapter retraction. From *in vivo* data for 18G needle (Fig. 3), we observe a sudden increase in main axial (F_z) force when the needle enters into the patient's skin [Fig. 3(a)]. The force continued increasing until about 8.5 mm of insertion (maximum force is about 9.2 N), then decreased because of relaxation in tissue/organ due to the

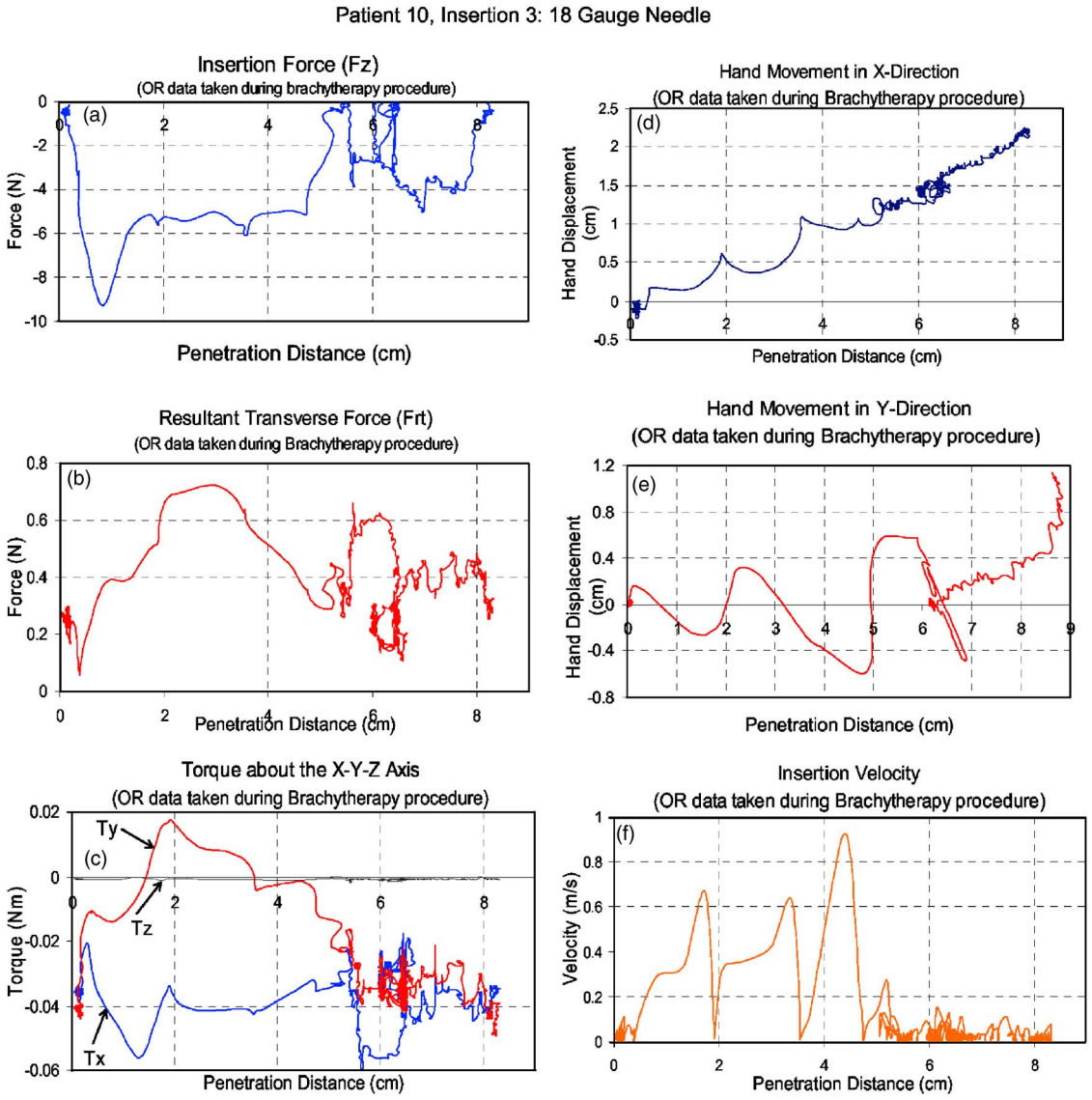

FIG. 3. Forces and motion profiles for 18G (1.27 mm in diameter) needle insertion in patient 10 during brachytherapy procedure in the OR.

surgeon pausing to confirm the needle penetration from US image. Again, the force started increasing when the needle touched the prostate capsule, producing a maximum capsule puncturing force of about 5.0 N, after which the force decreased to about 4 N. In Fig. 3(b) we noticed some transverse forces on the needle [resultant force (F_{rt}) of two transverse forces (F_x and F_y), maximum is about 0.71 N]. We notice some variations in these forces, during other insertions, which are due to the combination of lateral forces exerted by the movement of internal organ, heterogeneity of tissues, presence of template, prebending of needle, and inconsistency of human operation of the needle. However, the corresponding effect on (F_z) is ($F_{zf}=\mu F_{rt}$) quite small ($\mu \leqslant 0.2$ for steel-steel contact in wet condition, each needle is dipped into betadine solution just before insertion). Some of the undesired factors may be reduced if a robotic system is employed. However, we can eliminate neither the use of a needle support/guide, nor other factors such as tissue heterogeneity and movement of internal organ. Since the brachytherapy needles are thin and long (18G=1.27 mm, 17G =1.47 mm, 200 mm long), and inserted horizontally, they must be supported and guided to avoid sagging due to gravity and occasional bending due to high force at the start of insertion (puncturing skin). We also observed some torques about the x and y axes, but hardly any torque about the z axis [Fig. 3(c)]. These torques about the x and y axes are also combined effects of several factors such as tissue heterogeneity, presence of template, movement of internal organ, and transverse movement of the surgeon's hand. However, these torques are quite small. The transverse movements (in x and y directions) of the surgeon's hand have been captured using a 6 DOF EM sensor and have been presented in Figs. 3(d) and 3(e). The needle insertion velocity has been calculated using needle position data and recorded time stamps. We observe that the maximum needle insertion velocity at the initial stage is quite high (about 0.9 m/s), however, in the later stage of the penetration the velocity decreased significantly with some peaks [Fig. 3(f)]. This velocity profile was

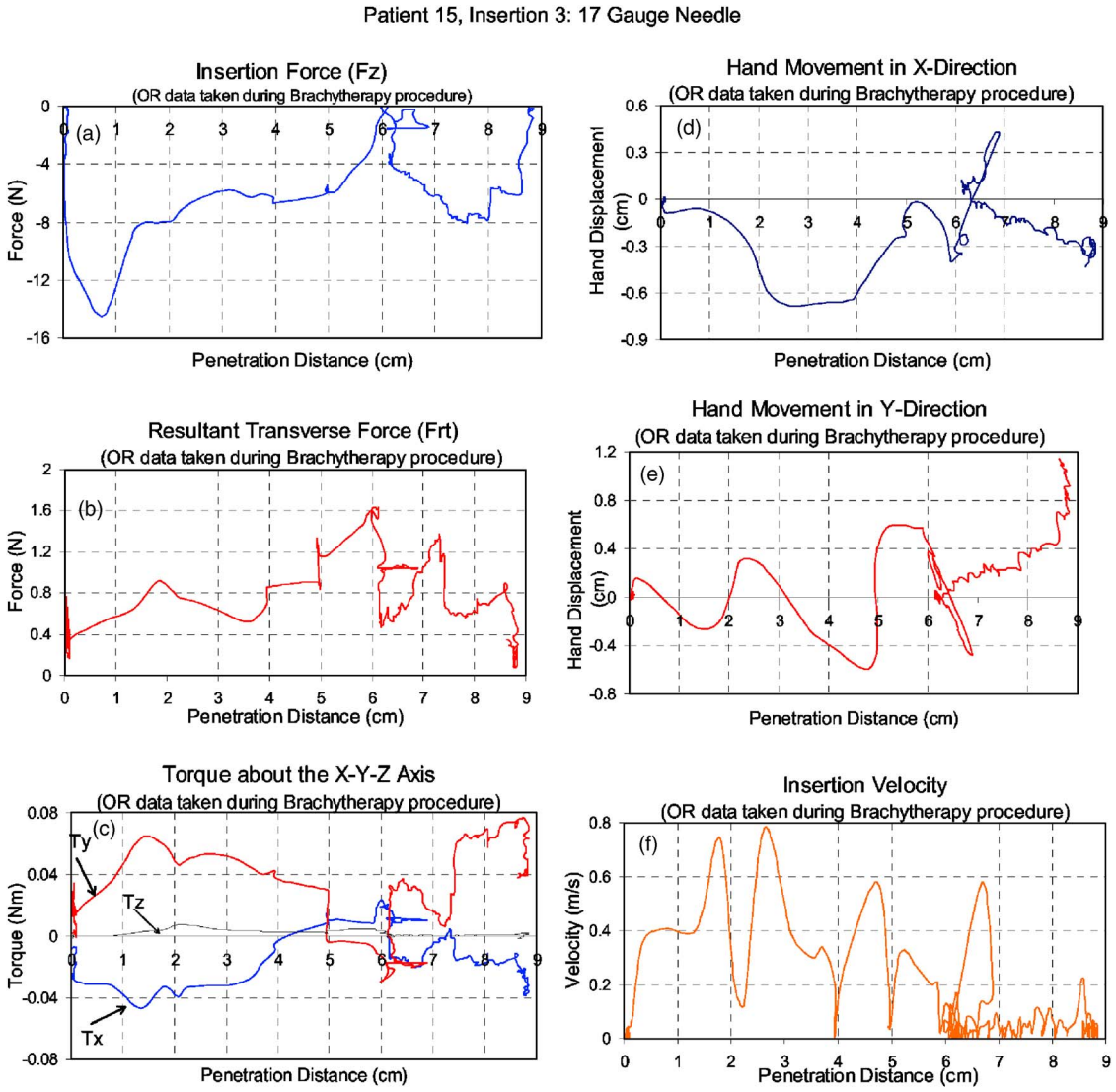

FIG. 4. Forces and motion profiles for a single 17G (1.47 mm in diameter) needle insertion in patient 15 during brachytherapy procedure in the OR.

remarkably different from many robotic needle insertions during *in vitro* experiments,[11,13,15] mainly due to the surgeon's pause to confirm the location of the needle with respect to the target. In the case of a robotic needle insertion into a patient, we may be unable to attain such a high velocity safely. However, we have not noticed any significant difference in measured parameters when the insertion velocities were small (ref. Table I, for patient 7 v_{max}=0.59 m/s, and for patient 8, v_{max}=0.4 m/s; these are done by another surgeon). It appears that at the relatively slower speed of needle that is suitable for clinical procedure, the force on the needle may not change significantly. However, further study is required to assess the effects of velocity modulation on insertion force and needle placement accuracy in living biological tissues, which tend to relax quite fast and to a significant degree.[9,12,21]

A representative data set (a single needle insertion into a patient) for 17G needle insertion has been presented in Fig. 4, from which we observe similar profiles of force and motion as noticed for 18G needles. However, the magnitude of forces, both F_z (insertion) and F_{rt} (resultant transverse), is remarkably high when compared to that of an 18G needle [Figs. 4(a) and 4(b)]. Here we observe that for a 17G needle the F_z is about 14.5 N and maximum F_{rt} is about 1.6 N, whereas on 18G needle the F_z is about 9.1 N and F_{rt} is about 0.71 N. A significant part of these force differences for two types of needles is attributed to the needle size differences, i.e., 18G (1.27 mm) and 17G (1.47 mm). Although the F_{rt} is high [Fig. 4(b)] in this particular insertion, we do not notice any significant movement of the surgeon's hand in a transverse direction, i.e., the x and y directions (Figs. 4(d) and 4(e)). However, we notice an average resultant transverse force less than 1.0 N for more than 75% of all the insertions. The same surgeon was asked to perform the same type of insertions (which is done during PSI) in the laboratory in a variety of animal tissue phantoms and soft material phantoms with and without the presence of a physical template that is used in the OR. It has been noticed that with the similar x-y motion of the hand, the extra friction force in-

TABLE I. Summary of *in vivo* data collected from the OR.

Needle	Patient No.	Max. force in perineum (N) (Avg./SD)	Max. force in prostate (N) (Avg./SD)	Max. velocity (m/s) (Avg./SD)
18G (1.27 mm) diamond tip needle	1	7.27/1.23	5.30/1.25	0.88/0.06
	2	7.90/1.20	6.27/0.52	0.73/0.24
	3	8.77/0.40	7.00/0.91	1.22/0.70
	4	10.39/2.53	10.14/4.11	1.44/0.51
	5	3.34/1.45	5.34/1.73	0.79/0.19
	6	13.94/5.03	6.06/3.36	1.95/1.10
	7	10.2/3.82	6.5/0.39	0.59/0.26
	8	8.49/2.63	5.38/0.77	0.4/0.29
	9	9.89/4.01	5.1/1.11	1.54/0.49
	10	8.46/0.92	5.83/2.36	0.98/0.31
	Patients 1–10	8.87/2.32	6.28/1.64	1.05/0.42
17G (1.47 mm) diamond tip needle	11	15.63/2.74	8.24/2.72	0.65/0.42
	12	16.85/4.45	5.95/0.64	1.17/0.40
	13	13.87/3.53	7.93/2.57	0.94/0.16
	14	15.26/4.61	5.72/0.95	0.98/0.01
	15	14.22/4.03	6.85/1.09	0.86/0.08
	16	16.58/2.79	8.14/2.17	1.67/0.74
	17	15.05/3.76	9.36/0.97	1.61/0.27
	18	13.89/1.10	11.91/3.110	1.27/0.36
	19	15.28/1.84	9.54/0.13	1.61/0.41
	20	19.11/0.96	10.61/0.89	2.27/2.10
	Patients 11–20	15.57/2.98	8.42/1.52	1.30/0.50

curred due to the presence of the template was about 1.0 N. Therefore, we think a major part of this higher force may be due to other factors mentioned before.

A summary of the *in vivo* data collected from all 20 patients has been presented in Table I. Average maximum forces before and after penetration into the prostate and also average maximum needle velocities have been tabulated here. The insertion force and velocity have been averaged for each patient (parameters were measured for two to three insertions per patient) along with the standard deviation (SD). Then for each type of needle (17G or 18G) the measured parameters have been averaged to find the overall average value. The maximum average forces outside and inside the prostate are 8.87 and 6.28 N, respectively, for 18G needles (patients 1–10). We notice a significant reduction of insertion force (about 29% less) when the needle is in the prostate. This reduction in force is mainly due to the presence of softer tissue. On the other hand, for 17G needle the insertion force dropped from 15.57 N outside the prostate to 8.42 N in the prostate (patients 11–20), a reduction of about 46%. This indicates that the force difference for 17G needle is more prominent compared to 18G needle. A comparison of overall maximum forces on 18G needle and 17G needle reveals that the perineum force on an 18G needle is about 43% less and the prostate force is about 25% less as compared to that on a 17G needle, suggesting a relatively less prominent effect of needle size in softer tissue. The average maximum velocity of 17G needle (1.3 m/s) was higher than that of 18G needle (1.05 m/s). This is due to the fact the surgeon anticipated larger force on the 17G needle and he tried to thrust the needle faster to compensate it. However, the effect of higher velocity does not have a significant effect on insertion force as seen in Table I, for patient 7 (v_{max}=0.59 m/s) and patient 8 (v_{max}=0.4 m/s), which were performed by another surgeon who inserted the needles slowly and gradually.

The maximum perineum/prostate force for all the insertions for both types of needles has been presented as a barchart in Fig. 5 (frequency versus force). The perineum force for 18G needle appears to have a good normal distribution with more variations, whereas the prostate force is slightly skewed to the right, but the distribution has less variation. On the other hand, for the 17G needle the force distribution is less like a perfect normal distribution, perineum force has a bimodal distribution, and the prostate force is more skewed to the right. In the case of the 17G needle, the main reason for more deviation of force distribution from a perfect normal distribution is that the 17G needles are used on those patients who have received prior hormonal treatment or EBRT and consequently have harder prostate and stiffer and thicker skins. However, the 95% confidence intervals for mean values of all the forces for both sets of needles appear to be quite compact (range is less than 2.5 N); collected data seem to be a good representative for the measured parameters. A significant variation is observed in perineum/prostate force for the 18G needle as compared to the 17G needle, probably because of several reasons as follows. The 18G needle is 13.5% smaller in diameter than the 17G needle. The presence of less stiffness in a needle will ultimately provide more variation due to the increased possibility of needle deviation. As mentioned above, the 18G needle is

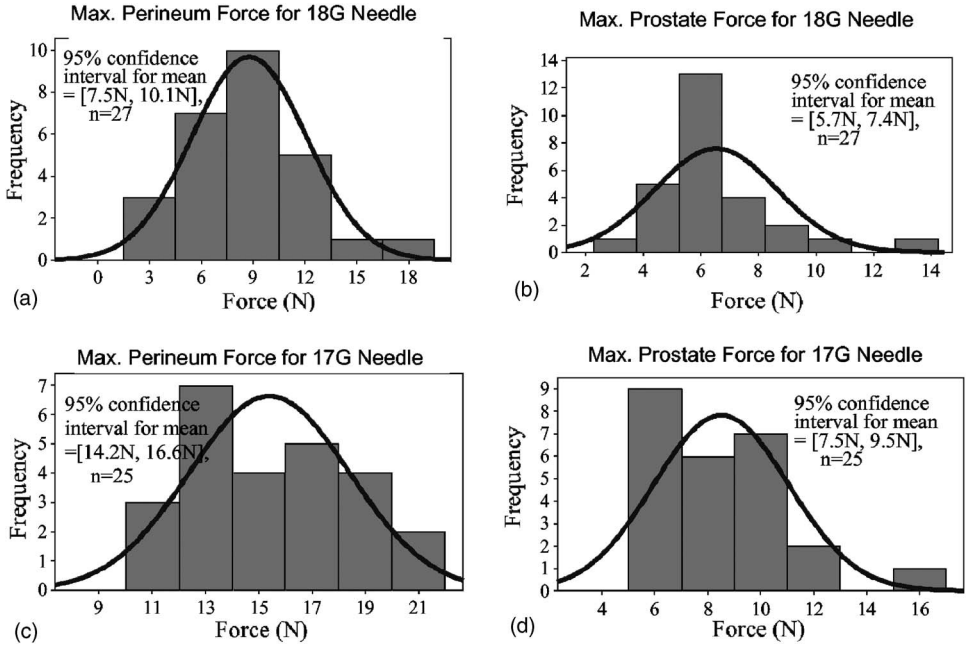

FIG. 5. Distribution of maximum force for all the insertions ($n=27$ for 18G needle and $n=25$ for 17G needle): (a) outside the prostate on 18 gauge needle, (b) inside the prostate on 18 gauge needle, (c) outside the prostate on 17 gauge needle, and (d) inside the prostate on 17 gauge needle.

commonly used for softer prostates and softer skinned patients. Therefore, we have less stiffness in both the needle as well as the prostate and surrounding tissue environment, consequently magnifying the amount of dissimilarity between each patient (being a heterogeneous environment). On the other hand, the 17G needle is stiffer and tends to be used in a more rigid environment (propertywise it might be giving more homogeneous characteristics) where more consistent data can be obtained. However, with increased number of data (52 insertions in 20 patients) it appears that force distribution of the 18G needle follows a better binomial distribution (Fig. 5).

To assess the effects of needle size on insertion force, we have performed some insertions into PVC phantoms with fixed boundary conditions. A significant difference in insertion forces was observed for 18G and 17G needles [Fig. 6(a), upon full insertion the difference was about 4 N in F_z, about 25% lower for 18G needle]. However, due to the increased flexibility of the 18G needle (which increased lateral contact with the template), the resultant transverse force was slightly higher when compared to the 17G needle [Fig. 6(b)]. From *in vivo* we found a difference of about 6.7 N (15.6−8.9 N, outside prostate) insertion force between 17G and 18G needles (Table I). In this phantom study we noticed about 4 N force difference between 17G and 18G needles [Fig. 6(a)], which is solely due to the needle size difference. Thus the 2.7 N (6.7−4 N) discrepancy in F_z is attributed to complex tissue/organ boundaries and their response to dissimilar needles, interaction between the template and the needle, and potentially other unknown factors.

IV. CONCLUSION

In this paper, we presented *in vivo* force-torque and needle insertion motion profile data collected from a total of 52 insertions in 20 patients during actual PSI procedures in the OR. The force-torque data have been collected using a 6 DOF force-torque sensor. The needle position has been recorded using a 6 DOF EM-based sensor. The *in vivo* data reveal that overall maximum average needle insertion force for an 18G needle is significantly lower (about 8.87 N/6.28 N) as compared to that of 17G needle (15.57 N/8.42 N). The average insertion velocity for 17G (1.3 m/s) is higher than that is for 18G (1.05 m/s). We also observe some transverse forces on the needles which were due to the combined effects of lateral forces exerted by the movement of internal organs, heterogeneity of tissues, presence of template, prebending of the needle, and lateral move-

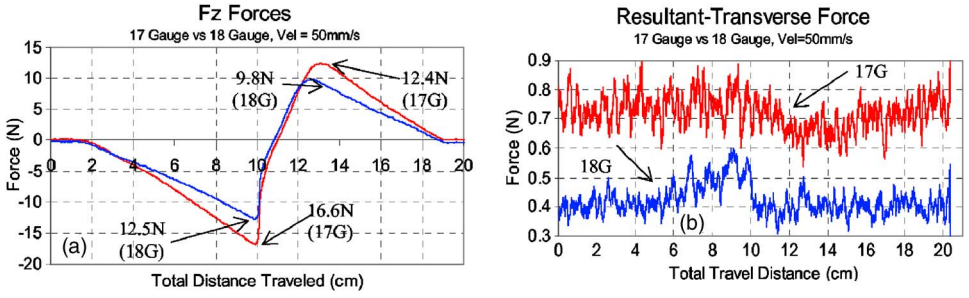

FIG. 6. Effect of needle size (18G vs. 17G) on insertion forces when inserted in PVC phantom.

ment of the surgeon's hand. Some of the undesired factors may be reduced if a robotic system is employed. But, the use of a needle guide and the existence of tissue heterogeneity, special anatomic conditions, and movement of internal organ cannot be eliminated. A second surgeon inserted needles at a slower speed (about 0.5 m/s) to perform multiple cases from which it appears that the velocity of needle insertion has minimal effect on the force. However, we are further investigating the effect of velocity modulation on needle insertion. For safety reasons, if the surgeon chooses to operate the robot at a lower speed, the amount of force the needle will experience may remain within the measured range.

It is intuitive that lower force will cause less deformation and displacement of internal tissue/organ and may create less trauma and edema to the patients. Thus, use of an 18G needle (1.27 mm in diameter) is more logical from a clinical point of view. However, the 17G needle (1.47 mm in diameter) is used based on some unavoidable patient-specific criteria for some patients who have undergone other treatments such as hormonal therapy, EBRT, etc., which makes the prostate harder and patients have thicker and stiffer skins.

The collected *in vivo* data impart useful insights into the force and torque on the needle, and needle velocity during actual brachytherapy procedure in the OR. This information will provide guidance in the design and control of a robotic system for prostate brachytherapy treatment with implantable radioactive seeds. The acquired knowledge also can be quite useful in developing predictive deformation model of the prostate and real-time adaptive control of the needle.

ACKNOWLEDGMENTS

This work is supported by the National Cancer Institute, under Grant No. R01 CA091763. We would like to thank Dr. Ganesh Palapattu, Maureen Kiernan, Kim Ferrari, Suzanne Vandeursen, and other clinical staff who helped us in collecting data in the OR.

[a]Electronic mail: tarun_podder@urmc.rochester.edu

[1]G. Fichtinger, "Robotically assisted prostate brachytherapy with transrectal ultrasound guidance—phantom experiments," Brachytherapy, **5**(1), 14–26 (2006).

[2]G. Fichtinger, T. L. DeWeese, A. Patriciu, A. Tanacs, D. Mazilu, J. H. Anderson, K. Masamune, R. Taylor, and D. Stoianovici, "System for robotically assisted prostate biopsy and therapy with intraoperative CT guidance," Acad. Radiol. **9**, 60–74 (2002).

[3]Z. Wei, G. Wan, L. Gardi, D. B. Bowney, and A. Fenster, "Robotic aided 3D TRUS guided intraoperative prostate brachytherapy," Proc. SPIE **5367**, 361–370 (2004).

[4]G. Wan, Z. Wei, L. Gardi, D. B. Downey, and A. Fenster, "Brachytherapy needle deflection evaluation and correction," Med. Phys. **32**(4), 902–909 (2005).

[5]J. Kettenbach *et al.*, "Robot-assisted biopsy using computed tomography-guidance: Initial results from in vitro tests," Invest. Radiol. **40**, 219–228 (2005).

[6]J. Kettenbach *et al.*, "Robot-assisted biopsy using ultrasound guidance: Initial results from *in vitro* tests," Eur. Radiol. **15**, 765–71 (2005).

[7]P. L. Williams and R. Warwick, *Gray's Anatomy*, 38th ed., edited by L. H. Bannister *et al.* (Churchill Livingstone, New York, 1995).

[8]S. P. DiMaio and S. E. Salcudean, "Needle insertion modeling and simulation," IEEE Trans. Rob. Autom. **19**(5), 864–875 (2003).

[9]T. K. Podder, D. P. Clark, D. Fuller, J. Sherman, W. S. Ng, L. Liao, D. J. Rubens, J. G. Strang, E. M. Messing, Y. D. Zhang, and Y. Yu, "Effects of velocity modulation during surgical needle insertion," in the *Proceedings of the 27th Annual International Conference of the IEEE Engineering in Medicine and Biology Society (EMBS)*, Shanghai, China, Sept. 2005, pp. 6766–6770.

[10]S. Okazawa *et al.*, "Hand-held steerable needle device," in *the MICCAI* (*LNCS*, Vol. 2879, pp. 223–230), Montreal, Canada, Nov. 2003.

[11]M. D. O'Leary, C. Simone, T. Washio, K. Yoshinaka, and A. M. Okamura, "Robotic needle insertion: Effect of friction and needle geometry," in *the Proceedings of the IEEE Int. Conference on Robotics and Automation*, Taipei, Taiwan, Sept. 2003, pp. 1774–1779.

[12]T. K. Podder, L. Liao, J. Sherman, V. Misic, Y. D. Zhang, D. Fuller, D. J. Rubens, E. M. Messing, J. G. Strang, W. S. Ng, and Y. Yu, "Assessment of prostate brachytherapy and breast biopsy needle insertions and methods to improve targeting accuracy," in the *IFMBE Proceedings of the 12th International Conference on Biomedical Engineering (ICBME)*, Vol. 12, Singapore, Dec. 2005.

[13]T. K. Podder, E. M. Messing, D. J. Rubens, J. G. Strang, R. A. Brasacchio, D. P. Clark, D. Fuller, L. Liao, W. S. Ng, and Y. Yu, "Evaluation of robotic needle insertion in conjunction with *in vivo* manual insertion in the operating room," in the *Proceedings of the 14th IEEE International Workshop on Robot and Human Interactive Communication (RO-MAN)*, Nashville, TN, Aug. 2005, pp. 66–72.

[14]C. Simone and A. M. Okamura, "Modeling of needle insertion forces for robot-assisted percutaneous therapy," in *the Proc. of the IEEE Int. Conference on Robotics and Automation*, Washington, DC, May 2002, pp. 2085–2091.

[15]A. M. Okamura, C. Simone, and M. D. O'Leary, "Force modeling for needle insertion into soft tissue," IEEE Trans. Biomed. Eng. **51**(10), 1707–1716 (2004).

[16]P. Brett, A. J. Harrison, and T. A. Thomas, "Scheme for the identification of tissue types and boundaries at the tool point for surgical needles," IEEE Trans. Inf. Technol. Biomed. **4**(1), 30–36 (2000).

[17]M. P. Ottensmeyer and J. K. Salisbury, "In vivo data acquisition instrument for solid organ mechanical property measurement," in *the MICCAI* (*LNCS*, Vol. 2208, pp. 975–982), Utrecht, Netherlands, Oct. 2001.

[18]K. Yan, W. S. Ng, K. V. Ling, T. I. Liu, Y. Yu, and W. Odell, "Literature review on needle guidance in soft tissue and preliminary work on smart needling," in the *Proceedings of IEEE Conference on Robotics, Automation and Mechatronics*, Singapore, 2004, pp. 49–54.

[19]H. Kataoka, T. Washio, M. Audette, and K. Mizuhara, "A model for relations between needle deflection, force, and thickness on needle penetration," in *the MICCAI* (*LNCS*, Vol. 2208, pp. 966–974), Utrecht, Netherlands, Oct. 2001.

[20]T. A. Kruoskop, T. M. Wheeler, F. Kaller, B. S. Garra, and T. Hall, "Elastic moduli of breast and prostate tissues under compression," Ultrason. Imaging **20**, 260–274 (1998).

[21]Y. C. Fung, *Biomechanics: Mechanical Properties of Living Tissues*, 2nd ed. (Springer-Verlag, New York, 1993).

[22]P. S. Wellman, R. D. Howe, E. Dalton, and K. A. Kern, "Breast tissue stiffness in compression is correlated to histological diagnosis," Technical Report, Harvard BioRobotics Laboratory (http://biorobotics.harvard.edu/pubs.html), Division of Engineering and Applied Science, Harvard University, 1999.

[23]I. Sakuma *et al.*, "*In vitro* measurement of mechanical properties of liver tissue under compression and elongation using a new test piece holding method with surgical glue," in *the IS4TM/LNCS*, Vol. 2673, pp. 223–230, 2003.

[24]A. Samani, J. Bishop, C. Luginbuhl, and D. B. Plewes, "Measuring the elastic modulus of ex-vivo small tissue samples," Phys. Med. Biol. **48**(4), 2183–2198, (2003).

[25]K. Matsumiya *et al.*, "Analysis of forces during robotic needle insertion to human vertebra," in *the MICCAI* (*LNCS*, Vol. 2878, pp. 271–278), Montreal, Canada, Nov. 2003.